Frequency of subjects without *SLC26A4* mutation alleles in the borderline enlargement subgroup was significantly higher than those in the aperture enlargement and aperture & midpoint enlargement subgroups ($P < 0.0125$). It tended to be higher than that in the midpoint enlargement subgroup but it was not statistically significant ($P = 0.021$) probably due to the small number of subjects in the midpoint enlargement subgroup (n=4).

SLC26A4 mutations and genotypes in association with EVA morphology in subject with Pendred syndrome or DFNB4

The types and locations of all the *SLC26A4* mutations in 34 subjects with Pendred syndrome or DFNB4 were shown in Table II and Fig. 3. Five splice site mutations (c.601-1G>A (intron 5), c.919-2A>G (intron 7), c.1614+1G>A (intron 14), c.1708-32_1708-16del (intron 15), c.1707+5G>A (intron 15)), one non-sense mutation (p.L743X), two insertion/deletion mutations (p.S551Ffs13, Q705Wfs18), and 14 missense mutations (p.S28G, p.P76S, p.A372V, p.N392Y, p.R409H, p.T410M, p.T527P, p.I529S, p.Y556C, p.V659L, p.D669E, p.F692L, p.T721M, p.H723R) were detected. These included four novel mutations, p.S28G (c.82A>G), p.D669E (c.2007C>A), p.F692L (c.2074T>C), and c.1708-32_1708-16del (marked * in Table II) based on the criteria for novel mutations in the present study (described in methods). Electropherograms of the novel mutations and conservation of the amino acid residues among various species are shown in Fig. 3B and C. NNSPLICE predicted

9

c.1708-32_1708-16del to decrease probability of acceptor site at exon 16 from 0.49 (for normal allele)

to 0.19 (for mutation allele), which is likely to cause aberrant splicing (Fig. 3C).

The list of subjects with two *SLC26A4* mutation alleles are shown in Table II. Analysis of

genotypes of *SLC26A4* mutation alleles in these subjects showed that 20 (59%) had non-truncating/

non-truncating genotypes, 13 (38%) had non-truncating/ truncating genotypes, and 1 (3%) had

truncating/ truncating genotypes (Fig. 4A). Comparison of the incidence of each genotype found no

significant statistical difference between the subgroups of EVA morphology (P = 1.000).

Characteristics of hearing loss in association with EVA morphology in subjects with Pendred

syndrome or DFNB4

The hearing levels, incidence of hearing fluctuation, and progression of hearing loss in subjects with

two *SLC26A4* mutation alleles are shown in Table II. Relation between the hearing level and EVA

morphology was examined in the ears of 34 subjects (68 ears) (Fig. 4B). Thirty-four ears (50%) had

profound hearing loss in total. No significant differences in the hearing levels were detected between

the subgroups of EVA morphology (P = 0.462). In order to exclude the effect of aging in this analysis,

we also stratified the subjects into two groups (age 0-9 and 10y or older) and conducted the same

analysis. These analyses also demonstrated the same results, indicating that the difference in ages

among subgroups did not affect distribution of subjects among different hearing levels (data not

10

shown). Next, the relation between hearing fluctuation and EVA morphology was investigated in 28

subjects for whom relevant audiometric data were available (Fig. 4C). Hearing fluctuations were

detected in 15 subjects (54%) in total, and no significant differences were noted in the incidence of

hearing fluctuations between the subgroups of EVA morphology ($P = 0.209$). Lastly, the relation

between progression of hearing loss and EVA morphology was analyzed in 29 subjects for whom

relevant clinical data were available (Fig. 4D). Twenty subjects (69%) had progressive hearing loss in

total, and the results showed no significant differences in the incidence of progressive hearing loss

between the subgroups of EVA morphology ($P = 0.207$).

DISCUSSION

Although a variety of EVA criteria using the midpoint and aperture diameters of the vestibular

aqueduct have been proposed to date,[1,6-10] our study is the first attempt to divide EVA into subgroups

based on the shape and size of the vestibular aqueduct, and the first to investigate the possible

relationship of these subgroups with genotypes and audiometric findings. *SLC26A4* mutations were

detected in 72% of the Japanese subjects with bilateral EVA. Among these *SLC26A4* mutations, four

mutations were novel. The discovery of these novel mutations would expand the *SLC26A4* mutation

spectrum, thereby contributing to a more accurate gene-based diagnosis of hearing loss with EVA.

11

Nearly all subjects with aperture, aperture & midpoint, and midpoint enlargement presented

SLC26A4 mutations, suggesting that subjects with these EVA subgroups are most likely to be

diagnosed with Pendred syndrome or DFNB4. On the other hand, only approximately 30% of subjects

with borderline enlargement had SLC26A4 mutation, which suggests that majority of subjects with

this EVA subgroups have a pathological mechanism other than Pendred syndrome or DFNB4.

None of the 47 EVA subjects enrolled in the present study had only a single SLC26A4 mutation

allele. This finding is a striking contrast with previous research reporting single SLC26A4 mutation

alleles in approximately one-third of Caucasian subjects with EVA.[3,4,20-22] This discrepancy might be

associated with Japanese subjects who were reported to have distinct spectrum of SLC26A4 mutations

from Caucasian subjects.[22] One possible explanation is that the development of EVA in the Caucasian

population may more frequently involve mutations in the introns or promoter regions of the SLC26A4

than that in the Japanese population. Another possibility is that Caucasian population may have higher

mutation frequencies in genes causing digenic hearing loss in association with heterozygous SLC26A4

mutations (e.g., KCNJ10 and FOXI1) than Japanese population.[23-25] The other possible explanation for

the discrepancy is that the present study registered only subjects with bilateral EVA, whereas previous

studies included those with unilateral hearing loss or unilateral EVA. This implicates the hypothesis

that biallelic mutations of SLC26A4 are more strongly associated with bilateral EVA.

Our analysis of subjects with SLC26A4 mutations revealed no significant difference in the

12

proportion of truncating and non-truncating *SLC26A4* mutations between subgroups of EVA

morphology. This suggests that, in addition to malfunction of the *SLC26A4* protein, environmental

factors or genes other than *SLC26A4* may contribute to variations in vestibular aqueduct morphology.

Some researchers argue that there is no significant relationship between the degree of the EVA and

the severity and progression of hearing loss and hearing fluctuations, while others propose that there is

a significant relationship.[26] In the present study, no significant differences were detected in the level,

fluctuation, and progression of hearing loss between the subgroups of EVA morphology, indicating

that characteristics of hearing loss cannot be predicted based on the EVA morphology in subjects with

Pendred syndrome or DFNB4.

CONCLUSION

Almost all the subjects with aperture, aperture & midpoint, and midpoint enlargement of EVA had

two *SLC26A4* mutation alleles, whereas more than two thirds of subjects with borderline enlargement

of EVA had no *SLC26A4* mutation alleles. Analysis of subjects with two *SLC26A4* mutation alleles

revealed no significant correlation between the morphologic subgroups of EVA and *SLC26A4*

genotypes or characteristics of hearing loss, suggesting that the subgroups of EVA morphology may be

associated with factors other than genotypes of *SLC26A4* mutations and that the subgroups of EVA

morphology are not a predictive factor for characteristics of hearing loss.

13

The American Laryngological, Rhinological and Otological Society, Inc.

ACKNOWLEDGEMENTS

14

REFERENCES

1. Madden C, Halsted M, Benton C, Greinwald J, Choo D. Enlarged vestibular aqueduct syndrome in

    the pediatric population. Otol Neurotol 2003; 24:625-632.

2. Madden C, Halsted M, Meinzen-Derr Jet al. The influence of mutations in the SLC26A4 gene on

    the temporal bone in a population with enlarged vestibular aqueduct. Arch Otolaryngol Head Neck

    Surg 2007; 133:162-168.

3. Pryor SP, Madeo AC, Reynolds JCet al. SLC26A4/PDS genotype-phenotype correlation in

    hearing loss with enlarged vestibular aqueduct (EVA): evidence that Pendred syndrome and

    non-syndromic EVA are distinct clinical and genetic entities. J Med Genet 2005; 42:159-165.

4. Azaiez H, Yang T, Prasad Set al. Genotype-phenotype correlations for SLC26A4-related deafness.

    Human Genet 2007; 122:451-457.

5. Choi BY, Stewart AK, Madeo ACet al. Hypo-functional SLC26A4 variants associated with

    nonsyndromic hearing loss and enlarged vestibular aqueduct: genotype-phenotype correlation or

    coincidental polymorphisms? Human mutation 2009; 30:599-608.

6. Valvassori GE, Clemis JD. The large vestibular aqueduct syndrome. Laryngoscope 1978;

    88:723-728.

7. Jackler RK, De La Cruz A. The large vestibular aqueduct syndrome. Laryngoscope 1989;

15

99:1238-1242.

8. Levenson MJ, Parisier SC, Jacobs M, Edelstein DR. The large vestibular aqueduct syndrome in children. A review of 12 cases and the description of a new clinical entity. Arch Otolaryngol Head Neck Surg 1989; 115:54-58.

9. Okumura T, Takahashi H, Honjo I, Takagi A, Mitamura K. Sensorineural hearing loss in patients with large vestibular aqueduct. Laryngoscope 1995; 105:289-293.

10. Vijayasekaran S, Halsted MJ, Boston M et al. When is the vestibular aqueduct enlarged? A statistical analysis of the normative distribution of vestibular aqueduct size. Am J Neuroradiol 2007; 28:1133-1138.

11. Smith SD, Harker LA. Single gene influences on radiologically-detectable malformations of the inner ear. J Commun Disord 1998; 31:391-408; quiz 409-310.

12. Everett LA, Glaser B, Beck JC et al. Pendred syndrome is caused by mutations in a putative sulphate transporter gene (PDS). Nat Genet 1997; 17:411-422.

13. Phelps PD, Coffey RA, Trembath RC et al. Radiological malformations of the ear in Pendred syndrome. Clin Radiol 1998; 53:268-273.

14. Usami S, Abe S, Weston MD, Shinkawa H, Van Camp G, Kimberling WJ. Non-syndromic hearing loss associated with enlarged vestibular aqueduct is caused by PDS mutations. Human Genet 1999; 104:188-192.

16

15. Reyes S, Wang G, Ouyang X et al. Mutation analysis of SLC26A4 in mainland Chinese patients with enlarged vestibular aqueduct. Am Acad Otolaryngol Head Neck Surg 2009; 141:502-508.

16. Exome Variant Server: http://evs.gs.washington.edu/EVS/

17. dbSNP: http://www.ncbi.nlm.nih.gov/snp/

18. Reese MG, Eeckman, FH, Kulp, D, Haussler, D. Improved Splice Site Detection in Genie. J Comp Biol 1997; 4:311-323.

19. Worrld Health Organization Grades of Hearing Impairment: http://www.who.int/pbd/deafness/hearing_impairment_grades/en/index.html

20. Albert S, Blons H, Jonard Let al. SLC26A4 gene is frequently involved in nonsyndromic hearing impairment with enlarged vestibular aqueduct in Caucasian populations. Eur J Hum Genet 2006; 14:773-779.

21. Campbell C, Cucci RA, Prasad Set al. Pendred syndrome, DFNB4, and PDS/SLC26A4 identification of eight novel mutations and possible genotype-phenotype correlations. Human mutation 2001; 17:403-411.

22. Tsukamoto K, Suzuki H, Harada D, Namba A, Abe S, Usami S. Distribution and frequencies of PDS (SLC26A4) mutations in Pendred syndrome and nonsyndromic hearing loss associated with enlarged vestibular aqueduct: a unique spectrum of mutations in Japanese. Eur J Hum Genet 2003; 11:916-922.

17

330

23. Madeo AC, Manichaikul A, Reynolds JCet al. Evaluation of the thyroid in patients with hearing loss and enlarged vestibular aqueducts. Arch Otolaryngol Head Neck Surg 2009; 135:670-676.

24. Yang T, Vidarsson H, Rodrigo-Blomqvist S, Rosengren SS, Enerback S, Smith RJ. Transcriptional control of SLC26A4 is involved in Pendred syndrome and nonsyndromic enlargement of vestibular aqueduct (DFNB4). Am J Hum Genet 2007; 80:1055-1063.

25. Yang T, Gurrola JG, 2nd, Wu Het al. Mutations of KCNJ10 together with mutations of SLC26A4 cause digenic nonsyndromic hearing loss associated with enlarged vestibular aqueduct syndrome. Am J Hum Genet 2009; 84:651-657.

26. Gopen Q, Zhou G, Whittemore K, Kenna M. Enlarged vestibular aqueduct: review of controversial aspects. Laryngoscope 2011; 121:1971-1978.

18

330

FIGURE LEGENDS

Fig. 1. Typical temporal bone CT images of the enlarged vestibular aqueduct (EVA) subgroups.

(A) aperture enlargement. (B) aperture & midpoint enlargement. (C) midpoint enlargement. (D)

borderline enlargement. The midpoint and external aperture of the vestibular aqueduct are indicated by

white and black arrows, respectively. As shown in the inset of (A), the midpoint diameter (fine dotted

line) and aperture diameter (coarse dotted line) were measured perpendicular to the long axis (white

solid line) of the vestibular aqueduct.

Fig. 2. Number of subjects with or without *SLC26A4* mutation alleles in each EVA subgroup.

Asteriscs; significant difference (P <0.0125)

Fig. 3. The location of each mutation in *SLC26A4*, the evolutionary conservation of the amino

acids ,and nucleotides affected by the novel missense and splice site mutations. (A) location of the

SLC26A4 mutations found in this study. Putative transmembrane regions are shown in black. N-term

G; sulfate transporter N-terminal domain with Gly motif, Sulf-T; Sulfate transporter family domain,

STAS; Sulphate transporter and anti-sigma factor antagonist domain. (B) electropherograms of the

novel mutations and the corresponding sequence from normal alleles. Note that the nucleotide

sequence of c.1708-32_1708-16del is shown reverse complementary. (C) upper; multiple alignments

19

of SLC26A4 protein orthologues at two non-contiguous regions. Arrows indicate affected amino

acids. Conserved amino acids are shaded in gray. lower; boundaries between the intron15 and

exon16 and deleted nucleotides are indicated at the bottom.

Fig. 4. Association of EVA subgroups with *SLC26A4* genotypes or characteristics of hearing loss in

subjects with biallelic *SLC26A4* mutations. (A) proportion of *SLC26A4* genotypes in subjects of each

EVA subgroup. (B) proportion of different hearing levels in ears of each EVA subgroup. (C)

prevalence of fluctuating hearing loss in subjects of each EVA subgroup. (D) prevalence of

progressive hearing loss in subjects of each EVA subgroup.

Table I. Criteria for the subgroups of enlarged vestibular aqueduct

Enlarged vestibular aqueduct subgroup	Midpoint diameter	External aperture diameter
Aperture enlargement	≧1.5 mm	Wider than midpoint
Aperture and midpoint enlargement	≧1.5 mm	Equal to midpoint
Midpoint enlargement	≧1.5 mm	Narrower than midpoint
Borderline enlargement	1.0 mm to <1.5mm	1.0 mm to <1.5mm

Table II. Types of SLC26A4 mutations and characteristics of hearing loss in 34 subjects with Pendred syndrome or DFNB4 by EVA subgroups.

EVA morhpology	diagnosis age of deafness (y)	age (y)	Allele 1 exon/intron	Allele 1 DNA change	Allele 1 amino acid change or splicing mutation	Allele 2 exon/intron	Allele 2 DNA change	Allele 2 amino acid change or splicing mutation	truncating/non-truncating	hearing level R/L** (dBHL)	fluctuation of hearing	progression of hearing loss
Aperture enlargement	0	1	Intron15	c.1707+5G>A	Splice site mutation	19	2106-2110dup5	Q705Wfs18	T/T	90/70#	-	+
	0	33	15	1652insT	S551Ffs13	19	c.2168A>G	p.H723R	T/N	95/95	-	+
	2	6	Intron7	c.919-2A>G	Splice site mutation	19	c.2168A>G	p.H723R	T/N	53.75/63.75	-	+
	0	27	Intron7	c.919-2A>G	Splice site mutation	19	c.2168A>G	p.H723R	T/N	98.75/100	+	+
	0	1	Intron15	c.1707+5G>A	Splice site mutation	19	c.2168A>G	p.H723R	T/N	85##	Unknown	+
	0	31	Intorn5	c.601-1G>A	Splice site mutation	19	c.2168A>G	p.H723R	T/N	73.75/60	+	+
	3	11	Intorn5	c.601-1G>A	Splice site mutation	19	c.2168A>G	p.H723R	T/N	70/87.5	+	+
	0	4	Intron15	c.1707+5G>A	Splice site mutation	2	c.82A>G*	p.S28G*	T/N	61.25/61.25	-	Unknown
	0	35	Intorn5	c.601-1G>A	Splice site mutation	10	c.1229C>T	p.T410M	T/N	80/73.75	+	+
	3	12	19	c.2168A>G	p.H723R	19	c.2168A>G	p.H723R	N/N	82.5/106.25	+	+
	3	3	19	c.2168A>G	p.H723R	19	c.2168A>G	p.H723R	N/N	62.5/73.75	-	-
	0	4	19	c.2168A>G	p.H723R	19	c.2168A>G	p.H723R	N/N	55/70	+	-
	0	2	19	c.2168A>G	p.H723R	19	c.2168A>G	p.H723R	N/N	37.5##	Unknown	Unknown
	0	1	19	c.2168A>G	p.H723R	19	c.2168A>G	p.H723R	N/N	102.5/115###	-	-
	0	0.5	10	c.1229C>T	p.T410M	19	c.2228T>A	p.L743X	N/N	73.75##	Unknown	Unknown
	0	1	9	c.1115C>T	p.A372V	10	c.1226G>A	p.R409H	N/N	92.5##	-	-
	0	20	19	c.2168A>G	p.H723R	14	c.1579A>C	p.T527P	N/N	97.5/101.25	-	-
	0	4	15	c.1667A>G	p.Y556C	14	c.1579A>C	p.T527P	N/N	77.5/75	-	+
	0	6	3	c.266C>T	p.P76S	14	c.1579A>C	p.T527P	N/N	17.5/93.75	-	+
	0	9	10	c.1174A.>T	p.N392Y	19	c.2162C>T	p.T721M	N/N	103.75/110	+	+
Aperture & midpoint enlargement	0	15	Intron15	c.1708-32_1708-16del*	Splice site mutation*	19	c.2168A>G	p.H723R	T/N	76.25/91.25	+	+
	0	9	Intron7	c.919-2A>G	Splice site mutation	17	c.2007C>A*	p.D669E*	T/N	100/100	+	-
	0	1	19	c.2168A>G	p.H723R	14	c.1579A>C	p.T527P	N/N	115##	-	-
	5	6	19	c.2168A>G	p.H723R	19	c.2168A>G	p.H723R	N/N	47.5/62.5	-	-
	1	2	19	c.2168A>G	p.H723R	19	c.2168A>G	p.H723R	N/N	105/93.75###	Unknown	Unknown
Midpoint enlargement	0	3	Intron7	c.919-2A>G	Splice site mutation	17	c.2007C>A*	p.D669E*	T/N	82.5/93.75####	+	+
	0	8	19	c.2168A>G	p.H723R	18	c.2074T>C*	p.F692L*	N/N	75/115	+	+
	7	10	19	c.2168A>G	p.H723R	19	c.2168A>G	p.H723R	N/N	60/15	+	+
	0	35	10	c.1229C>T	p.T410M	17	c.1975G>C	p.V659L	N/N	97.5/87.5	+	+

	0	5	Intron7	c.919-2A>G	Splice site mutation	19	c.2168A>G	p.H723R	T/N	73.75/77.5	+	+
	2	2	intron14	c.1614+1G>A	Splice site mutation	10	c.1229C>T	p.T410M	T/N	55##	Unknown	Unknown
Borderline enlargement	4	4	19	c.2168A>G	p.H723R	19	c.2168A>G	p.H723R	N/N	106.25/88.75####	Unknown	+
	0	6	14	c.1586T>G	p.I529S	19	c.2168A>G	p.H723R	N/N	80/66.25	-	-
	4	14	10	c.1229C>T	p.T410M	19	c.2168A>G	p.H723R	N/N	118.75/58.75	+	+

*, candidate novel mutation;   **, value without slash indicates binaural stimulus;   #, ABR;   ##, COR;   ###, ASSR ;   ####, play
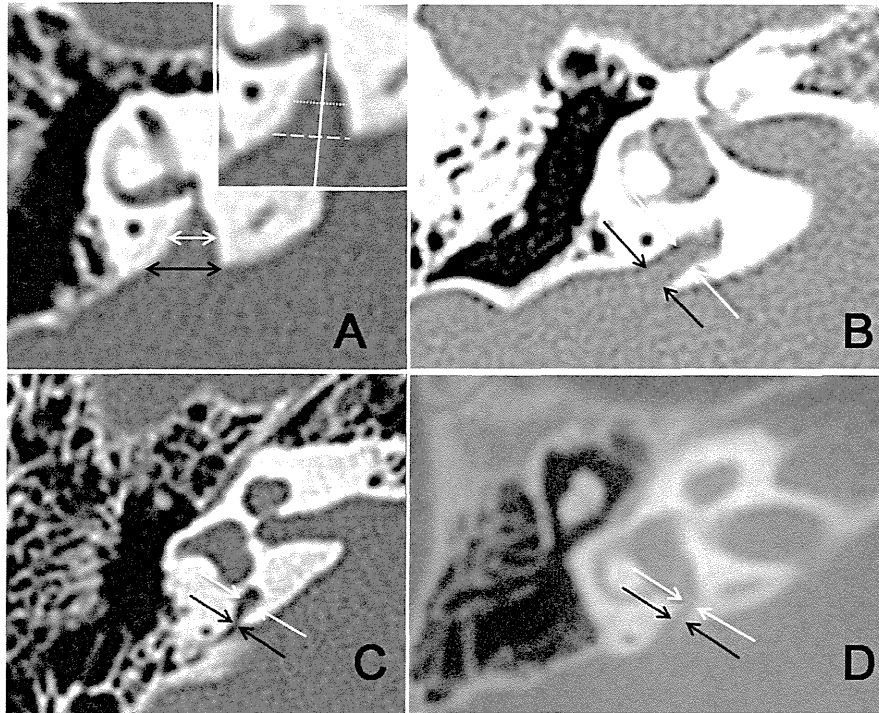
Fig. 1

Typical temporal bone CT images of the enlarged vestibular aqueduct (EVA) subgroups.
(A) aperture enlargement. (B) aperture & midpoint enlargement. (C) midpoint enlargement. (D) borderline enlargement. The midpoint and external aperture of the vestibular aqueduct are indicated by white and black arrows, respectively. As shown in the inset of (A), the midpoint diameter (fine dotted line) and aperture diameter (coarse dotted line) were measured perpendicular to the long axis (white solid line) of the vestibular aqueduct.

184x160mm (150 x 150 DPI)
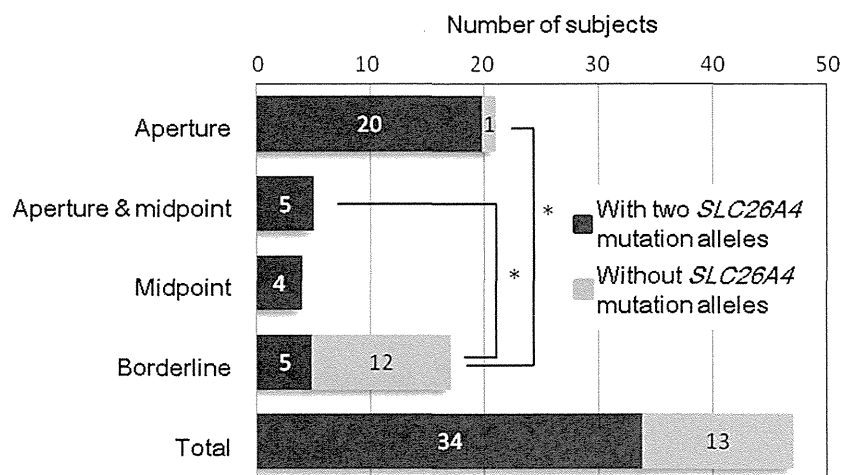
Fig.2

Number of subjects with or without SLC26A4 mutation alleles in each EVA subgroup. Asteriscs; significant difference (P <0.0125)
130x100mm (150 x 150 DPI)
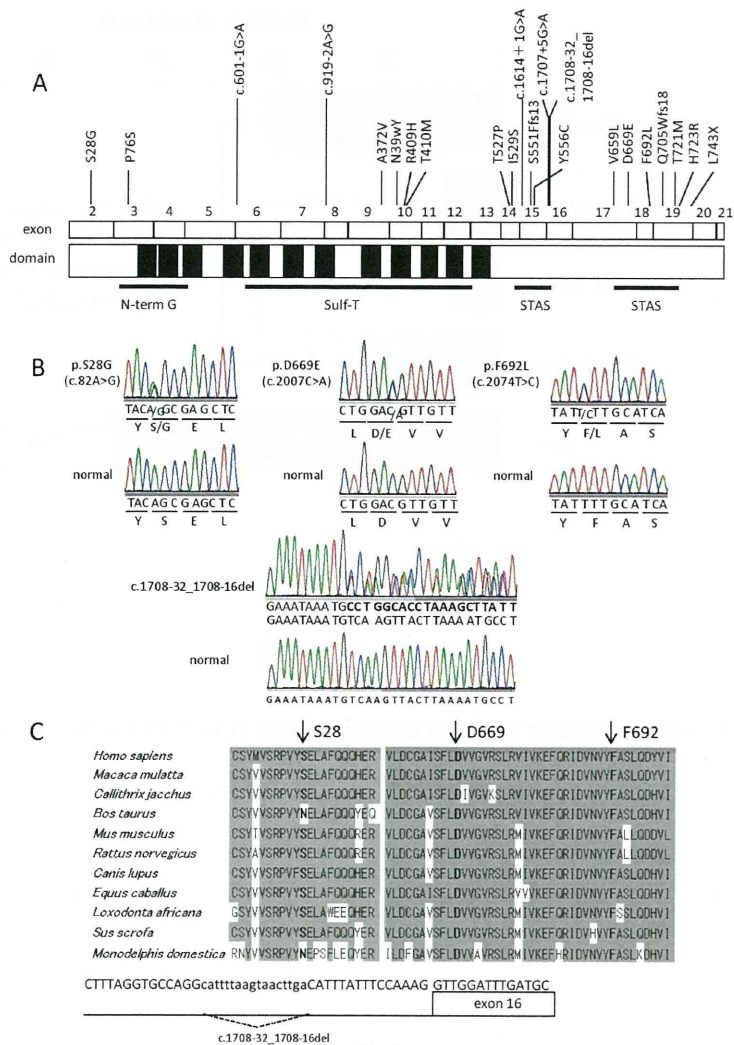
Fig.3

The location of each mutation in SLC26A4, the evolutionary conservation of the amino acids ,and nucleotides affected by the novel missense and splice site mutations. (A) location of the SLC26A4 mutations found in this study. Putative transmembrane regions are shown in black. N-term G; sulfate transporter N-terminal domain with Gly motif, Sulf-T; Sulfate transporter family domain, STAS; Sulphate transporter and anti-sigma factor antagonist domain. (B) electropherograms of the novel mutations and the corresponding sequence from normal alleles. Note that the nucleotide sequence of c.1708-32_1708-16del is shown reverse complementary. (C) upper; multiple alignments of SLC26A4 protein orthologues at two non-contiguous regions. Arrows indicate affected amino acids. Conserved amino acids are shaded in gray. lower; boundaries between the intron15 and exon16 and deleted nucleotides are indicated at the bottom.
176x252mm (150 x 150 DPI)
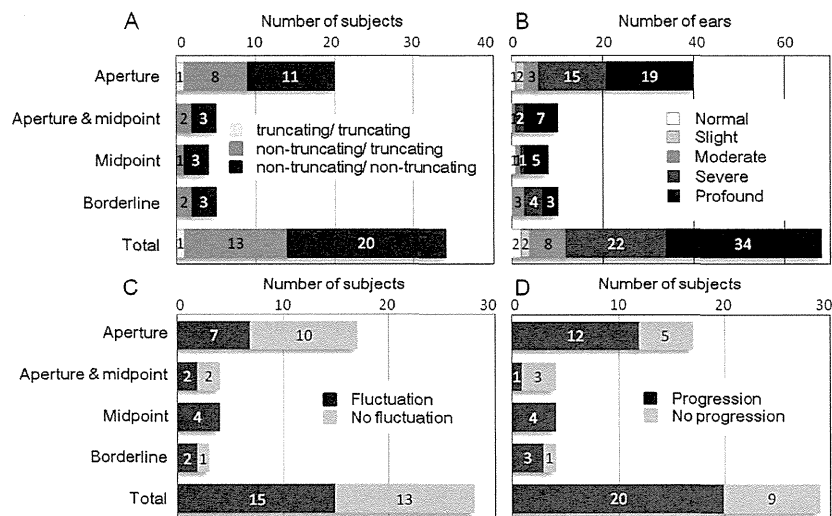
Fig.4

Association of EVA subgroups with SLC26A4 genotypes or characteristics of hearing loss in subjects with biallelic SLC26A4 mutations. (A) proportion of SLC26A4 genotypes in subjects of each EVA subgroup. (B) proportion of different hearing levels in ears of each EVA subgroup. (C) prevalence of fluctuating hearing loss in subjects of each EVA subgroup. (D) prevalence of progressive hearing loss in subjects of each EVA subgroup.
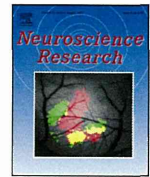193x141mm (150 x 150 DPI)

Long-lasting changes in the cochlear K+ recycling structures after acute energy failure

Yoichiro Takiguchi [a,b,c], Guang-wei Sun [b,1], Kaoru Ogawa [c], Tatsuo Matsunaga [b,*]

[a] Department of Otolaryngology, Eiju General Hospital, 2-23-16 Higashi-ueno, Taito-ku, Tokyo 110-8645, Japan
[b] The Laboratory of Auditory Disorders, National Institute of Sensory Organs, National Tokyo Medical Center, 2-5-1 Higashigaoka, Meguro-ku, Tokyo, 152-8902, Japan
[c] Department of Otolaryngology, School of Medicine, Keio University, 35 Shinanomachi, Shinjuku-ku, Tokyo, 160-8582, Japan

ARTICLE INFO

ABSTRACT

Fibrocytes in the cochlear lateral wall and spiral limbus play an important role in transporting K+ and have the capacity of self-renewal. We showed that acute energy failure in the rat cochlea induced by local administration of the mitochondrial toxin 3-nitropropionic acid (3NP) caused hearing loss in a concentration-dependent manner, mainly due to degeneration of cochlear fibrocytes. We produced long-lasting profound cochlear damage in this model by modifying the 3NP administration protocol and observed morphological changes at 16 weeks after the administration. In the spiral ligament, severe degeneration of fibrocytes was observed in the basal turn, and the levels of the Na,K-ATPase alpha and beta1 subunits and of NKCC1 were decreased in these cells, whereas connexin 26 (Cx26) level increased in the type 1 fibrocytes adjacent to the stria vascularis. In the stria vascularis, levels of Kir4.1 and L-PGDS decreased. In the spiral limbus, severe degeneration of fibrocytes was observed in the middle and basal turns, but NKCC1 and Cx26 were still found in the center of the limbus in the middle turn. These results indicate long-lasting changes in the cochlear lateral wall and spiral limbus, which may compensate for damaged K+ recycling and protect cells from ATP shortage.

© 2013 Elsevier Ireland Ltd and the Japan Neuroscience Society. All rights reserved.

1. Introduction

Sudden sensorineural hearing loss (SSNHL) is a common cause of otologic emergencies encountered by otorhinolaryngologists, and it has a reported recovery rate of 30–60% (Conlin and Parnes, 2007). SSNHL becomes fixed after 8–12 weeks from onset (Ito et al., 2002), and there is no effective therapy for SSNHL after that period (Slattery et al., 2005). The majority of patients with persistent SSNHL have a perceived handicap associated with tinnitus and hearing loss (Chiossoine-Kerdel et al., 2000). The prevailing theories for the cause of SSNHL are ischemia or viral infection of the cochlea. The cells of the inner ear are considered to be highly susceptible to mitochondrial dysfunction (Fischel-Ghodsian et al., 2004; Pickles, 2004; Hsu et al., 2005), which likely underlies the

susceptibility of the inner ear to acute energy failure such as cochlear ischemia (Seidman et al., 1999).

The cochlear lateral wall plays important roles in the physiology of hearing, including the transport of K+ to generate an endocochlear potential in the endolymph that is essential for transduction of sound by hair cells (Wangemann, 2002). The spiral ligament in the lateral wall consists of five types of fibrocytes based on their structural features, immunostaining patterns, and general location. The stria vascularis consists of three types of cells, including basal cells, intermediate cells, and marginal cells (Spicer and Schulte, 1996) (Fig. 1). It has been suggested that the recycling of K+ back into the stria vascularis is critical for these functions. It has also been postulated that the cochlear ion transport system, which is essential for hearing, consists of extracellular flow through the scala tympani and scala vestibuli, and transcellular flow through the organ of Corti, supporting cells, and cells of the lateral wall. According to this theory, type 2 and type 4 fibrocytes resorb K+ from the surrounding perilymph and from outer sulcus cells via Na,K-ATPase and NKCC1 (Na-K-Cl cotransporter isoform 1). The K+ are then transported to type 1 fibrocytes, stria basal cells, and intermediate cells through gap junctions and then secreted into the intrastrial space through the Kir4.1 channel (an inwardly rectifying K+ channel). The secreted K+ are incorporated into marginal cells by Na,K-ATPase and NKCC1 and are finally secreted into the